Lineage-specific expansion and loss of tyrosinase genes across platyhelminths and their induction profiles in the carcinogenic oriental liver fluke, *Clonorchis sinensis*

SEON-HEE KIM *and* YOUNG-AN BAE*

Department of Microbiology, Gachon University College of Medicine, 191 Hambakmoe-ro, Yeonsu-gu, Incheon 21936, Republic of Korea

(*Received 1 December 2016; revised 4 May 2017; accepted 4 May 2017; first published online 6 June 2017*)

SUMMARY

Tyrosinase provides an essential activity during egg production in diverse platyhelminths by mediating sclerotization of eggshells. In this study, we investigated the genomic and evolutionary features of tyrosinases in parasitic platyhelminths whose genomic information is available. A pair of paralogous tyrosinases was detected in most trematodes, whereas they were lost in cyclophyllidean cestodes. A pseudophyllidean cestode displaying egg biology similar to that of trematodes possessed an orthologous gene. Interestingly, one of the paralogous tyrosinases appeared to have been multiplied into three copies in *Clonorchis sinensis* and *Opisthorchis viverrini*. In addition, a fifth tyrosinase gene that was minimally transcribed through all developmental stages was further detected in these opisthorchiid genomes. Phylogenetic analyses demonstrated that the tyrosinase gene has undergone duplication at least three times in platyhelminths. The additional opisthorchiid gene arose from the first duplication. A paralogous copy generated from these gene duplications, except for the last one, seemed to be lost in the major neodermatans lineages. In *C. sinensis*, tyrosinase gene expressions were initiated following sexual maturation and the levels were significantly enhanced by the presence of O_2 and bile. Taken together, our data suggest that tyrosinase has evolved lineage-specifically across platyhelminths related to its copy number and induction mechanism.

Key words: *Clonorchis sinensis*, tyrosinase, gene evolution, tyrosinase induction, bile, oxygen.

INTRODUCTION

Dioxygen and its chemical derivatives such as superoxide anions, hydroxyl radicals and hydrogen peroxide emerged in the earth's biosphere as by-products of cellular metabolism. Living organisms have developed various defence mechanisms to cope with these highly aggressive chemicals. Antioxidant enzymes including superoxide dismutase, catalase, peroxidase and oxygenases are a primary defence against reactive oxygen molecules (reviewed in Jaenicke and Decker, 2004). Tyrosinases (EC 1·14·18·1) are also contributable to the removal of oxygen by incorporating the molecule into organic compounds. The enzymes catalyse hydroxylation of tyrosine into dihydroxyphenylalanine (DOPA; monophenol oxidase activity) and oxidation of DOPA into DOPA quinone (diphenol oxidase activity) (Sánchez-Ferrer *et al*. 1995). Tyrosinases contain a binuclear copper active site and form the type-3 copper protein family together with catecholoxidases, which mediate oxidation of *o*-diphenols to quinones, and hemocyanins, which act as oxygen carriers (Decker and Tuczek, 2000; Burmester, 2002; Aguilera *et al*. 2013).

Tyrosinases are ubiquitously distributed across a variety of taxa ranging from bacteria to mammals, which demonstrates their early origin in the evolution of life (van Gelder *et al*. 1997; Andreini *et al*. 2008; Aguilera *et al*. 2013). Nonetheless, the proteins exhibit substantial difference in primary structure, which affects the substrate binding pocket and the substrate accessibility, and the composition of functional domains related to the taxonomical positions of donor organisms (van Gelder *et al*. 1997; Aguilera *et al*. 2013). This structural heterogeneity seems to play an important role in the functional diversification of tyrosinases including roles in pigmentation, innate immunity, sclerotization and wound healing (Aguilera *et al*. 2013 and references therein). Based on the structural conservation and domain architecture, tyrosinases are categorized into three subclasses, namely secreted α-, cytosolic β-, and membrane-bound γ-subclasses (Aguilera *et al*. 2013). The multifaceted tyrosinase genes might be descendent from a common ancestor *via* two ancient gene duplication events in metazoan animals, which was followed by the differential loss and expansion of the multiplied genes in specific phyla (Burmester, 2002; Esposito *et al*. 2012; Aguilera *et al*. 2013).

In parasitic trematodes, tyrosinases provide enzymatic activity essential for the formation of eggshells (Cordingley, 1987). The proteins are produced in mature vitellocytes and packed within a secreting vacuole, termed vitelline droplet, together with eggshell precursor proteins (Smyth and Halton, 1983). Following activation in the ootype, tyrosinases

* Corresponding author: Department of Microbiology, Gachon University College of Medicine, 191 Hambakmoe-ro, Yeonsu-gu, Incheon 21936, Korea. E-mail: yabae03@gmail.com

doi:10.1017/S003118201700083X

convert tyrosine residues on eggshell proteins into DOPA quinones. The DOPA quinones are then cross-linked to other amino acids such as tyrosine and lysine on adjacent proteins to form the sclerotized eggshell (Cordingley, 1987). The cross-linking reactions are accompanied by changes in the colour and autofluorescence of the eggshell components (Kelly and von Lichtenberg, 1970). Trematode tyrosinases display high degrees of similarity in their structural properties and spatial expression patterns, as has been demonstrated in *Schistosoma mansoni* (Fitzpatrick *et al*. 2007), *Schistosoma japonicum* (Cai *et al*. 2009), *Clonorchis sinensis* (Bae *et al*. 2013), and *Paragonimus westermani* (Bae *et al*. 2015).

Clonorchis sinensis is a digenean trematode that parasitizes the bile ducts of mammalian hosts including humans. Human infection (i.e. clonorchiasis) occurs by eating raw or undercooked freshwater fish containing infective metacercariae of the parasite. Clonorchiasis is prevalent in several areas of Asian countries such as China, Korea and Vietnam, where it causes great socio-economic and public health burdens (Lun *et al*. 2005). Approximately 35 million people suffer from the parasitic disease (Keiser and Utzinger, 2009). In addition to the typical clinical symptoms including abdominal pain, mechanical obstruction of the hepatobiliary ducts, cholangiectasis and biliary stones (Lun *et al*. 2005), chronic infection of *C. sinensis* in humans appears to lead to high incidences of cholangiocarcinoma (Bouvard *et al*. 2009; Shin *et al*. 2010). The egg of parasitic helminthes is not only responsible for maintenance of the parasitic life cycle and their population growth, but is also an etiological factor that induces chronic inflammation (Cho *et al*. 2000; Hoffmann *et al*. 2002; Fairfax *et al*. 2012). Therefore, understanding of the evolution of egg formation-related genes and their induction profiles in response to particular host environments is essential for the development of strategies to control infectious diseases caused by egg-laying parasites.

In this study, we analysed tyrosinase genes isolated in the genomes of *C. sinensis* and other digenean trematodes by focusing on the characterization of their evolutionary history. Cestode and planarian genomes were included in the primary screening to form comparative groups. Induction profiles of individual paralogous genes were also examined in *C. sinensis* during its maturation/development and in response to the exogenous stimuli specific in the infected host environment such as O_2 and bile.

MATERIALS AND METHODS

Genome- and transcriptome-wide survey of tyrosinase genes

The draft genome sequences of multiple species selected for this study, including that of *C. sinensis*, were downloaded from each of the web-based databases indicated in Supplementary Fig. 1. The databases included the Chinese National Human Genome Center at Shanghai (http://lifecenter.sgst.cn/schistosoma/cn/schistosomaCnIndexPage.do), GenBank (http://www.ncbi.nlm.nih.gov/), GeneDB (http://www.genedb.org/), Joint Genome Institute (JGI, http://genome.jgi-psf.org), Sanger Institute (http://www.sanger.ac.uk/) and SmedGD (http://smedgd.neuro.utah.edu/). The genomic sequences were queried with the tyrosinase sequences of *Neurospora crassa* (CAE81941), *C. sinensis* (GAA 27975, GAA32069, GAA48882 and GAA48883; Bae *et al*. 2013), *Caenorhabditis elegans* (NP_491709) and human (NP_000363) through a series of searches with the stand-alone and web-based Basic Local Alignment Search Tool (BLAST). Transcriptomic and proteomic databases were similarly surveyed in their respective databases or in GenBank. Redundant expressed sequence tag (EST) sequences were aligned with one another using the CAP3 program (Huang and Madan, 1999) to construct a consensus contig. Nucleotide sequences obtained from the transcriptome and/or EST databases were further used as queries for the BLAST searches of genomic sequences. Finally, the retrieved proteins or coding DNA sequences (CDSs) were filtered to eliminate redundant sequences, by comparing chromosomal gene sequences matched to the respective molecules. Otherwise, a 95% similarity cutoff was considered for speciation of paralogous proteins. Open reading frames (ORFs) and translated amino acid sequences of all transcripts were predicted using ORF Finder (http://www.ncbi.nlm.nih.gov/). The similarity patterns and specific HMM profiles of the putatively translated amino acid sequences were analysed using BLASTp (*E*-value cutoff 1×10^{-5}) and InterProScan (version 5.0; http://www.ebi.ac.uk/Tools/pfa/iprscan5/), respectively. The hydrophobic signal peptides and transmembrane domains were examined using SignalP (http://www.cbs.dtu.dk/services/SignalP/) and TMPred (http://www.ch.embnet.org/software/TMPRED_form.html).

The identities (or names) of tyrosinases are distinguished by their protein accession numbers for convenience. For those genes, of which protein products were not retrieved, the accession numbers of expressed sequence tags are presented as their unique identities.

Phylogenetic analyses

The full amino acid sequences of the trematode tyrosinase-like proteins were aligned using MUSCLE (Edgar, 2004) and manually optimized using GeneDoc (Nicholas and Nicholas, 1997). The alignment was examined with ProtTest (version 2.4; Abascal *et al*. 2005) to determine the

https://doi.org/10.1017/S003118201700083X Published online by Cambridge University Press

best-fit model of protein sequence evolution. Based on the LG + G + I model as selected by ProtTest, a phylogenetic analysis was conducted using Bayesian inference implemented in MrBayes (version 3.2.6; Ronquist and Huelsenbeck, 2003) through the server at CIPRES Science Gateway V.3.3 (https://www.phylo.org/). Bayesian posterior probabilities were calculated by the Markov chain Monte Carlo (MCMC) method (2×10^6 generations, two runs with four chains, sampling every 1000 generations). The default values of the program were used to set the other parameters. A 50% majority-rule consensus tree was made with multiple phylogenetic trees to determine the posterior probabilities at different nodes. In addition, a maximum likelihood tree was constructed with PhyML (version 3.1; Guindon *et al*. 2010) by selecting identical substitution model. Branch support was inferred using the non-parametric Shimodaira-Hasegawa-like approximate likelihood ratio test (SH-aLRT) provided by PhyML. The resulting tree was displayed by TreeView (Page, 1996). Position-by-position evolutionary rates were estimated using the MEGA program (Tamura *et al*. 2013).

Analysis of exon-intron architectures and chromosomal synteny

Chromosomal DNA sequences of tyrosinase genes were extracted from genomic databases of donor organisms by web-based or stand-alone BLAST searches using CDSs of the respective genes. The exon-intron architectures were determined by aligning the genomic sequences with their CDSs. The accuracy of exon-intron boundaries were verified by confirming the presence of the splice site consensus sequence (GT-AG rule; Mount, 1982). The intron sites were compared to one another by referencing their positions in the sequence alignment of tyrosinase proteins, which was used in the phylogenetic analysis. The insertional phase of each intron relative to the reading frame was also examined (phase 0, between two consecutive codons; 1, between the first and second bases of a codon; 2, between the second and third bases of a codon).

Chromosomal segments or scaffolds encompassing the tyrosinase gene loci were retrieved from the genome browsers of *Schmidtea mediterranea* (SmedGD version 3.1; http://smedgd.neuro.utah.edu/) and *S. mansoni* (SchistoDB versions 3.0 [http://schistodb.net/schisto/] or Sanger Institute). Genome browsers in GenBank were scanned to obtain the chromosomal tyrosinase maps in *C. sinensis* and *Opisthorchis viverrini*. The nucleotide sequences of these segments were compared with those of *C. sinensis* in a pairwise manner using the BL2Seq program at NCBI (expect threshold: 0·001 for comparison between *C. sinensis* and *O. viverrini* sequences; 10 in other cases). GenBank proteomic databases of the respective species were also examined with the amino acid sequences of *C. sinensis* proteins detected in the retrieved segments (BLASTp algorithm; *E*-values $< 1 \times 10^{-6}$). A match of target species with the highest BLAST score was considered to be syntenic, if it occupied a region near tyrosinase in the corresponding chromosomal segments. The relative position and orientation of the proposed syntenic genes were also compared during the analysis.

Expression profiles of C. sinensis *tyrosinase genes*

Clonorchis sinensis metacercariae, which were collected from freshwater fish in an area of Korea, were administered orally into the stomach of Sprague-Dawley rats through a gavage needle (150 metacercariae per rat). Worms were collected from the rat's bile ducts at regular intervals from 4 to 140 days post-infection (dpi). Protocols for *C. sinensis* infection, maintenance of animals and recovery of the parasite under anaesthesia were approved by the Institutional Review Board of Gachon University (protocol number GIACUC-R2014005). Animals were housed in accordance with guidelines from the Association for the Assessment and Accreditation of Laboratory Animal Care (Thailand).

Total RNAs were extracted from *C. sinensis* worms (>30 worms/stage) using QIAzol solution and an RNeasy Mini kit (Qiagen, Hilden, Germany). Following removal of contaminating DNAs using an RNase-free DNase (New England Biolabs, Ipswich, MA), the RNAs were used in the complementary DNA (cDNA) synthesis with the iScript cDNA synthesis kit (Bio-Rad, Munich, Germany). Relative amounts of tyrosinase transcripts in the cDNA samples were estimated *via* quantitative real-time polymerase chain reaction (qPCR) with gene-specific primers (Supplementary Table S1). The *C. sinensis* β-actin gene (DF143505) was selected as a reference gene. The qPCR was conducted using the SYBR Green Master Mix and the CFX96 detection system following the manufacturer's instructions (Bio-Rad Laboratories, Hercules, CA). Control reactions without cDNA samples were included and melt curve analyses were performed to ensure the presence of a single amplicon. Each reaction was conducted in triplicate and the results were presented as mean ± standard deviation (S.D.). The relative expression level of each gene was calculated against the reference β-actin gene ($2^{-\Delta C_T}$; Livak and Schmittgen, 2001). Student's *t* tests were used for statistical analysis. A probability level (*P* value) of <0·05 was considered to be statistically significant.

Live 28-day-old *C. sinensis* worms (10 worms/group) were incubated with RPMI-1640 media (phenol red- and serum-free, pH 7·2) supplemented with various amounts of bile salts (0·01, 0·02 and 0·04%; Sigma-Aldrich, Oakville, ON, Canada) at 37

https://doi.org/10.1017/S003118201700083X Published online by Cambridge University Press

°C in 5%-CO_2 incubators. Using N_2 gas, the O_2 levels in the incubators were equilibrated to 1, 5 and 20%, respectively, during the incubation period. After 8 h incubation, the fold change in expression of tyrosinase genes was calculated with respect to that in un-incubated *C. sinensis* worms ($2^{-\Delta\Delta C_T}$ method; Livak and Schmittgen, 2001) *via* the quantitative reverse transcription PCR (qRT-PCR) method as described above. The 7- and 12-day-old worms (50 worms per group) were similarly incubated for 8 h under the 20%-O_2 conditions. Total RNAs were extracted from the worms, as well as from un-incubated worms of the same ages. The RNA samples were used in the qRT-PCR analysis to estimate the relative expression levels of tyrosinase genes ($2^{-\Delta C_T}$ method).

RESULTS

Tyrosinase genes in the platyhelminth genomes

The tyrosinase genes in the draft genomes of parasitic flatworms were analysed by a series of BLAST searches. In addition to the four genes described in our earlier work (Bae *et al*. 2013), a partial sequence encoding a further tyrosinase (GAA54899) was detected in the *C. sinensis* genome (Trematoda: Opisthorchiida; see also Aguilera *et al*. 2013). *Schistosoma mansoni* and *S. japonicum* (Trematode: Strigeidida) genomes encoded two paralogous genes, as were described in previous reports (Fitzpatrick *et al*. 2007; Cai *et al*. 2009). Additional proteins detected in the proteomic databases of these parasites were either allelic variants (identity values >95%) or simple redundant versions. The redundancy was verified by overlapping the genomic loci of two proteins in question. In *O. viverrini* (Trematoda: Opisthorchiida), five genes appeared to comprise tyrosinase paralogs (XP_009170910-1, XP_009170910-2, XP_009170911, XP_009173140 and XP_009169523; see next section), whereas *Fasciola hepatica* (Trematoda: Plagiorchiida) contained two tyrosinase genes (CCMX01034015 and CCMX01024173). Similar to the fifth *C. sinensis* tyrosinase, *O. viverrini* gene encoding the XP_009169523 protein was found to be partially determined. No tyrosinase gene was retrievable from the cestodes, including *Echinococcus granulosus, Echinococcus multilocularis, Taenia solium* (Cestoda: Cyclophyllidea: Taeniidae) and *Hymenolepis microstoma* (Cestoda: Cyclophyllidea: Hymenolepididae). However, a protein identified in the GenBank database of *Spirometra erinaceieuropaei* (AGC74039; Cestoda: Diphyllobothriidea: Diphyllobothriidae) showed strong structural similarity to the γ-subclass tyrosinases (*E*-values < 8×10^{-60} in a BLASTp search).

The draft genome and transcriptome shotgun assembly (TSA)/EST databases of *S. mediterranea* (Platyhelminthes: Turbellaria: Tricladida) were also queried to obtain tyrosinase sequence information. Multiple transcripts detected in the planarian TSA/EST databases were assigned to six tyrosinase genes (GAKN01000997, GAKN01006835/GAKN01006427, GAKN01001049, GAKN01005471, GAKN01007889/GAKN01004968 and JN983828/AY067481). The chromosomal loci of these genes were mapped to different genomic contigs (contig numbers 7108, 5589, 1071, 2182, 116 and 627, respectively). The current GenBank databases of other turbellarians did not include any gene/protein orthologous to the *S. mediterranea* tyrosinases. Multiple γ-subclass tyrosinases were identified in other metazoan taxa such as *Capitella teleta* (Annelida), *Saccoglossus kowalevskii* (Hemichordata), *Ciona intestinalis* (Tunicata) and *Branchiostoma floridae* (Cephalochordata), as well as species in the Craniata (see next section). Of these, *C. intestinalis* and *S. kowalevskii* contained additional genes homologous to α- and/or β-subclass tyrosinases. All the proteins identified in other organisms shown in Supplementary Fig. 1, including *C. elegans* (Nematoda), *Daphnia pulex* (Crustacea), *Lottia gigantean* (Mollusca) and *Nematostella vectensis* (Cnidaria), exhibited much higher similarity to the *C. elegans* protein (NP_491709; σ-subclass), which was in agreement with previous studies (Esposito *et al*. 2012; Aguilera *et al*. 2013; Bae *et al*. 2013). No tyrosinase homolog was identified in the genomes of *Strongylocentrotus purpuratus* (Echinodermata), *Trichoplax adhaerens* (Placozoa) and *Monosiga brevicollis* (Choanoflagellata). Interestingly the basal metazoan species *Suberites domuncula* (Demospongiae) possessed a tyrosinase gene of γ-subclass (CAE01389).

Phylogenetic relationships among platyhelminth tyrosinases

The primary structures of platyhelminth tyrosinases were compared with those of other γ-subclass tyrosinases and tyrosinase-related proteins. The full amino acid sequences of these proteins, rather than narrow-region restrictions, were thoroughly aligned (data not shown; for examples, see Bae *et al*. 2013, 2015). These proteins displayed similarities in their domain architecture, which comprised the Cys-rich epidermal growth factor-like domain (ELD) and a binuclear copper centre (Aguilera *et al*. 2013; Bae *et al*. 2013). Hydrophobic amino acids were primarily detected in the N- (signal peptide) and C-terminal (transmembrane domain) ends of tyrosinase-like proteins identified in the sponge and deuterostomians with a few exceptions. However, the C-terminal transmembrane domain was absent in the majority of the platyhelminth proteins. In addition to the annelide proteins, only a single *S. mediterranea* protein (JN983828) contained the transmembrane domain. The structural analysis further suggested that one of the *O. viverrini* proteins (XP_009170910) was an artificial concatemer comprising two distinct polypeptide sequences. Unique identities of these ligated

https://doi.org/10.1017/S003118201700083X Published online by Cambridge University Press

proteins, annotated as XP_009170910-1 and XP_009170910-2, were confirmed by the isolation of ESTs, specifically matched to the respective proteins (Ov_Contig3473/Ov_Contig396 and OV1_c1641). After removal of gaps (coverage cutoff 95%), the alignment was used in the phylogenetic analyses (380 amino acid positions; Supplementary File 1).

The relative evolutionary rate of each amino acid position differed in the trimmed alignment, while the rates were substantially low in the Cu(B) domain (Fig. 1). A Bayesian phylogenetic tree rooted with the *S. domuncula* protein (CAE01389) separated lophotrochozoan proteins from their deuterostomian homologs (posterior probabilities 0·83 and 0·99; Fig. 2). The lophotrochozoan tyrosinases were distinctly grouped according to their donor organisms at the phylum level (Annelida *vs* Platyhelminthes; posterior probabilities 1·00). Tyrosinases identified in platyhelminths were divided into two major clades, which were designated P_clade 1 and P_clade 2 (posterior probabilities 0·99 and 1·00), of which the later clade further split into multiple sub-clades; most of the trematode proteins comprised two paraphyletic sub-clades (P_clade 2-A and P_clade 2-B; posterior probabilities 1·00), while the *C. sinensis* GAA54899 and *O. viverrini* XP_009169523 proteins belonged to the more ancient P_clade 1. Two *S. mediterranea* proteins were included in the P_clade 2-B (GAKN01006835; posterior probability 1·00) and P_clade 1 (JN983828; posterior probability 0·99), respectively. Meanwhile, a pair of *S. mediterranea* proteins (P_clade 2-C; posterior probability 1·00) showed polytomic relationships with the subclades P_clade 2-A and P_clade 2-B. Genes encoding the two remaining *Schmidtea* proteins (GAKN01005471 and GAKN01007889) seemed to be originated from a series of gene duplication, which had occurred during an early evolutionary phase of the P_clade 2 lineage. The deuterostomian proteins other than those of *S. kowalevskii* were clustered into either the tyrosinase (TYR) or tyrosinase-related protein (TYRP) clades. A member(s) of TYRP clade was not identified in *S. kowalevskii*. In a maximum-likelihood tree, these tyrosinase proteins showed phylogenetic relationships similar to those observed in the Bayesian tree (Supplementary Fig. 2).

Chromosomal features of tyrosinase genes

Chromosomal sequences of the major trematode genes composed of three exons and two introns, of which positions and phases were tightly conserved among these orthologs (P_clade 2-A and P_clade 2-B; Fig. 3). The *S. mediterranea* genes closely related to the sub-lineages possessed introns at orthologous positions, whereas Smed-GAKN01000997 and Smed-GAKN01006835 were found to have gained a third intron in their 3′- and 5′-region, respectively. The exon-intron architectures were significantly different in the other *S. mediterranea* genes (GAKN01005471, GAKN01007889 and JN983828), while the JN983828 gene shared two orthologous introns with the P_clade 1 lineage genes of *C. sinensis* (GAA54899) and *O. viverrini* (XP_009169523). Genes identified in other taxa showed respective conservation patterns related to the phylogenetic positions of donor organisms. Instances of intron conservation across the animal taxa were also observed in the structural comparison. Interestingly, *Capitella* genes shared an intron with the most ancestral *S. mediterranea* gene (JN983828; Fig. 3).

The nucleotide sequences of genomic scaffolds occupied by tyrosinase genes were compared between *C. sinensis* and other platyhelminths using BL2Seq (Fig. 4). *Clonorchis sinensis* scaffold (DF142916) containing tyrosinases of the P_clade 2-A lineage displayed a significant similarity to the counterpart sequence of *O. viverrini* (NW_008751818; 87% nucleotide identity over 400-kb stretch). BLASTp searches revealed that four genes residing near tyrosinases have syntenic relationships in these parasites (E-values $< 2 \times 10^{-96}$, blue arrows in upper panel of Fig. 4). Relative orientations of these syntenic genes were also preserved in the homologous blocks. Of the three tyrosinase genes, two genes were separated by approximately 11 kb- and 15 kb-agenic regions in *C. sinensis* and *O. viverrini*, respectively, whereas the third gene was located opposite in the first intron of the other tyrosinase gene (green box in Fig. 4). Furthermore, these liver flukes possessed conserved nucleotide blocks approximately 260 kb (76% identity, six syntenic genes) and 190 kb (81% identity, two syntenic genes) in length that encompassed tyrosinase genes of the P_clade 2-B and P_clade 1 lineages, respectively. In *S. mansoni*, only the large subunit ribosomal protein L31e gene appeared to form short synteny with the P_clade 2-A tyrosinase (E-value 1×10^{-36}), whereas no nucleotide block with considerable identity to those of *C. sinensis* and *O. viverrini* was detected (expected threshold 10). No tyrosinase-containing synteny was recognized in the genomic contigs of *S. mediterranea* (Fig. 4).

Expression profiling of C. sinensis tyrosinase genes

The transcriptional profiles of tyrosinase genes during the development/maturation of *C. sinensis* were examined by qRT-PCR. As shown in Fig. 5, the mRNA transcripts of tyrosinase genes were not readily detected in metacercariae and juveniles younger than 10 days old, whereas expression of most genes were induced exponentially in 12- to 22-day-old worms, after which the expression levels were gradually decreased. The relative expression levels significantly differed among the five paralogous genes at each developmental stage; GAA27975 and

https://doi.org/10.1017/S003118201700083X Published online by Cambridge University Press

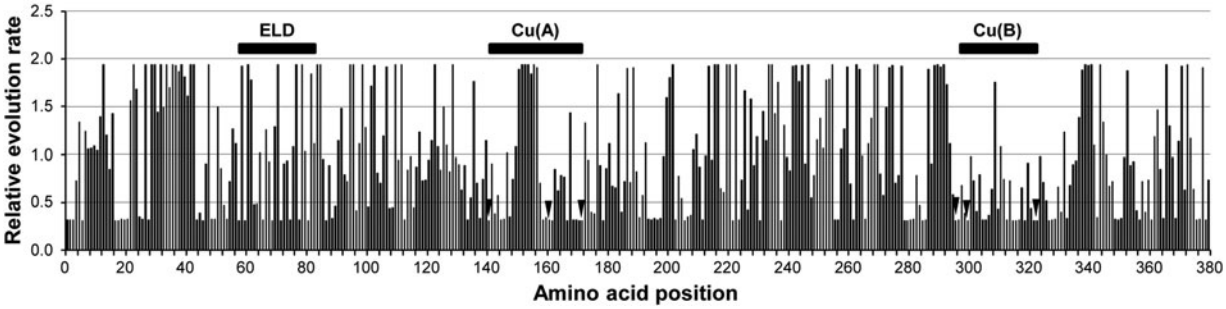

Fig. 1. Position-by-position evolutionary rates of platyhelminth tyrosinase sequences. The amino acid sequences of platyhelminth tyrosinases were aligned and used to estimate the relative evolutionary rate at each amino acid position by using the maximum likelihood algorithm of MEGA. Black bars mark the positions of major functional domains including the epidermal growth factor-like domain (ELD) and the binuclear copper center [Cu(A) and Cu(B)]. Arrowheads indicate histidine residues that comprise the active centre.

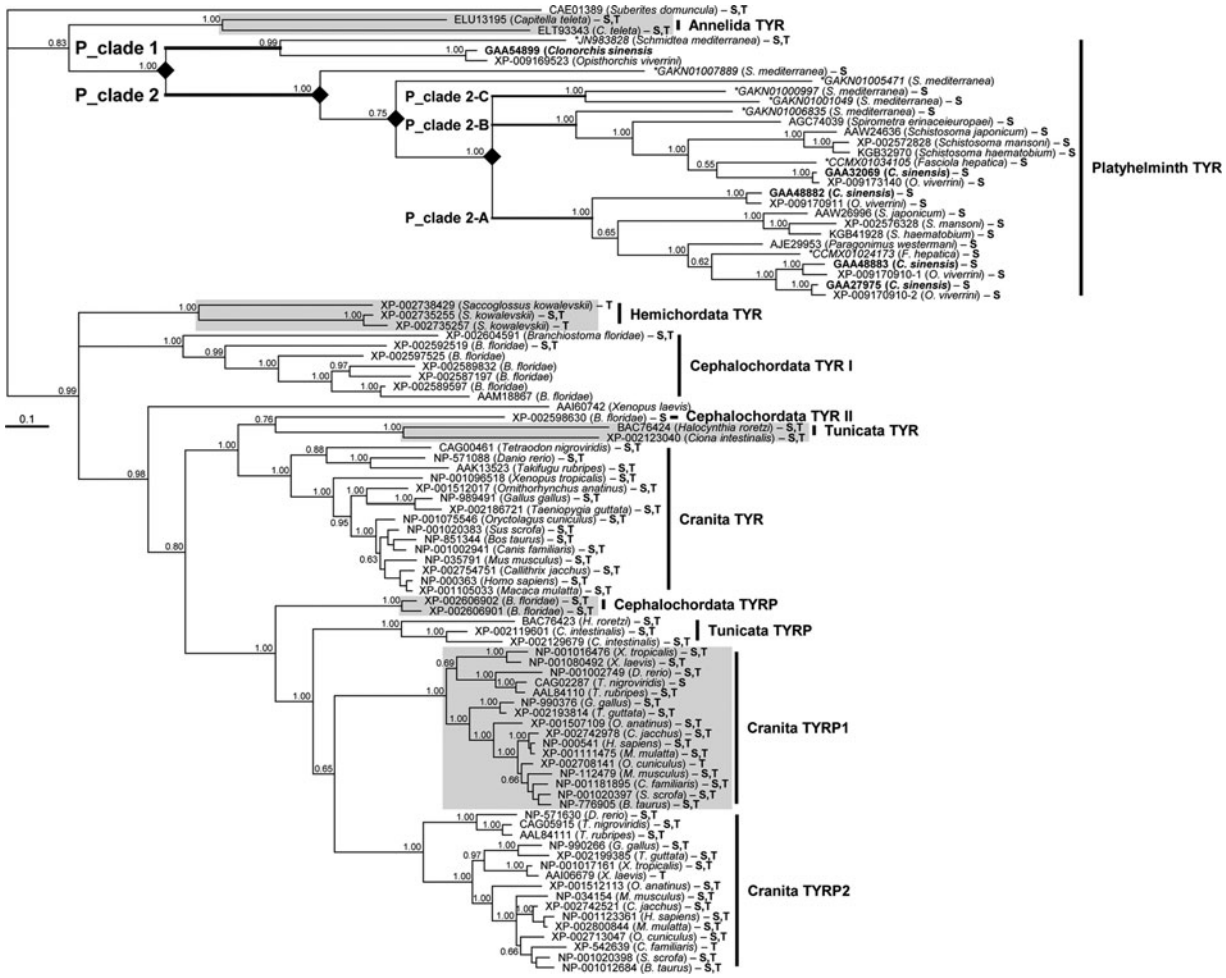

Fig. 2. Bayesian phylogenetic tree of tyrosinases (TYR) and tyrosinase-related proteins (TYRP) in animal taxa including *Clonorchis sinensis* (bold letters). The 50% majority-rule consensus tree was constructed using the alignment of their amino acid sequences with MrBayes and rooted with the *Suberites domuncula* protein (CAE01389). The identity of each protein was distinguished by its GenBank accession number and the scientific name of its donor organism in parenthesis. Italicized accession numbers with asterisks denote proteins, for which sequence information was predicted using mRNA sequences. The numbers at the nodes represent Bayesian posterior probabilities. Proteins conserving a signal peptide and transmembrane domain are marked with 'S' and 'T', respectively. P_clade 1 and 2 categorize members of two major lineages detected in the subtree of platyhelminth proteins. Solid diamonds indicate nodes that represent the gene duplication events, which may have occurred in the common ancestors of turbellarians and neodermatans.

https://doi.org/10.1017/S003118201700083X Published online by Cambridge University Press

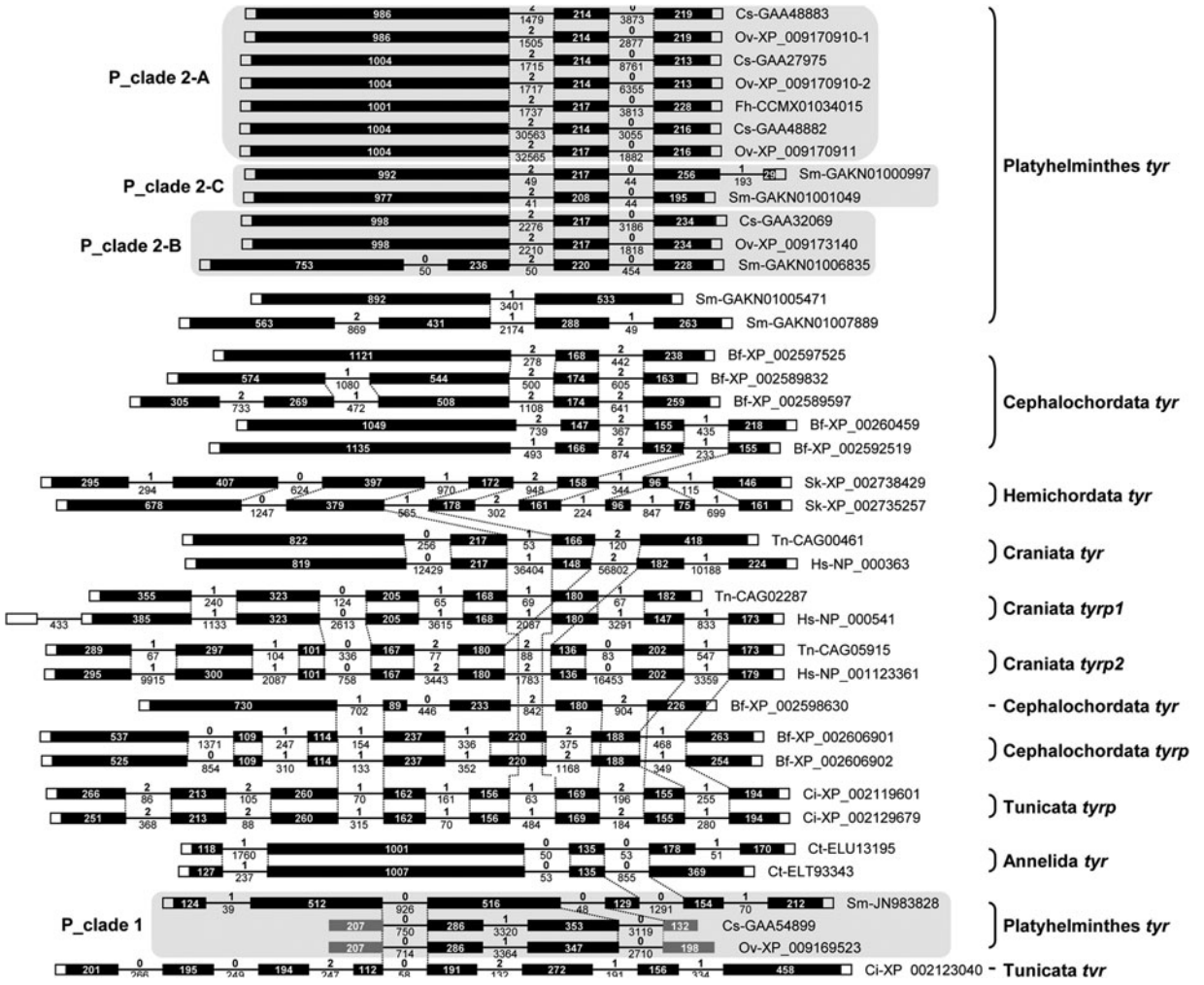

Fig. 3. Exon-intron composition of tyrosinase (*tyr*) and tyrosinase-related protein (*tyrp*) genes. Coding DNA sequences are presented with solid squares in proportion to their relative sizes and the 5′- and 3′-untranslated regions are marked with open squares with a voluntary length. The partially determined exons in the P_clade 1 genes of *Clonorchis sinensis* and *Opisthorchis viverrini* are marked with grey squares. Intervening introns are indicated by solid lines with a fixed length. The lengths of exons and introns in bp are indicated at the corresponding positions. Numerals 0, 1 and 2 show the phases of each intron. Orthologous introns that share positioning and phase among tyrosinase genes are indicated by vertical dotted lines Species abbreviations used are Cs, *Clonorchis sinensis*; Ov, *Opisthorchis viverrini*; Fh, *Fasciola hepatica*; Sm, *Schmidtea mediterranea*; Bf, *Branchiostoma floridae*; Sk, *Saccoglossus kowalevskii* ; Tn, *Tetraodon nigroviridis*; Hs, *Homo sapiens*; Ci, *Ciona intestinalis*; and Ct, *Capitella teleta*.

GAA54899 displayed the highest and the lowest expression levels, respectively (e.g. 720·4 ± 100·57 *vs* 0·1 ± 0·02 in 22-day-old worms). The minor GAA54899 gene maintained a basal expression level throughout development/maturation.

The effects of exogenous factors including O_2 and bile on the expression levels of tyrosinase genes were examined *via* the *ex host* treatment of live worms and subsequent qRT-PCR analyses. In 12-day-old worms treated with 20% O_2 for 8 h, expression levels of the main tyrosinase genes were slightly increased compared with those in un-incubated control worms (1·17–1·33 fold; P value < 0·05), although this exogenous factor did not affect tyrosinase genes in 7-day-old worms (Fig. 6A). Interestingly, this O_2-dependent induction pattern significantly changed in the fully mature *C. sinensis* adults (4-wk-old) (Fig. 6B). No significant gene induction was observed in worms treated with the atmospheric level of O_2. However, expression of the major tyrosinase genes was significantly enhanced up to 5-fold in worms treated with low oxygen levels (1 and 5%). The fold changes in expression of these genes (GAA4882 > GAA48883 > GAA32069 > GAA27975) were inversely proportional to their relative transcriptional activities at that developmental stage (GAA4882 < GAA48883 < GAA32069 < GAA27975; Fig. 5). In addition to O_2, bile also affected tyrosinase genes; treatment of bile enhanced and repressed tyrosinase gene expression under 5/20%- and 1%-O_2 conditions, respectively, in a dose-dependent manner. In contrast to these highly inducible genes, the low-expressed GAA54899 gene did not significantly respond to treatment with

https://doi.org/10.1017/S003118201700083X Published online by Cambridge University Press

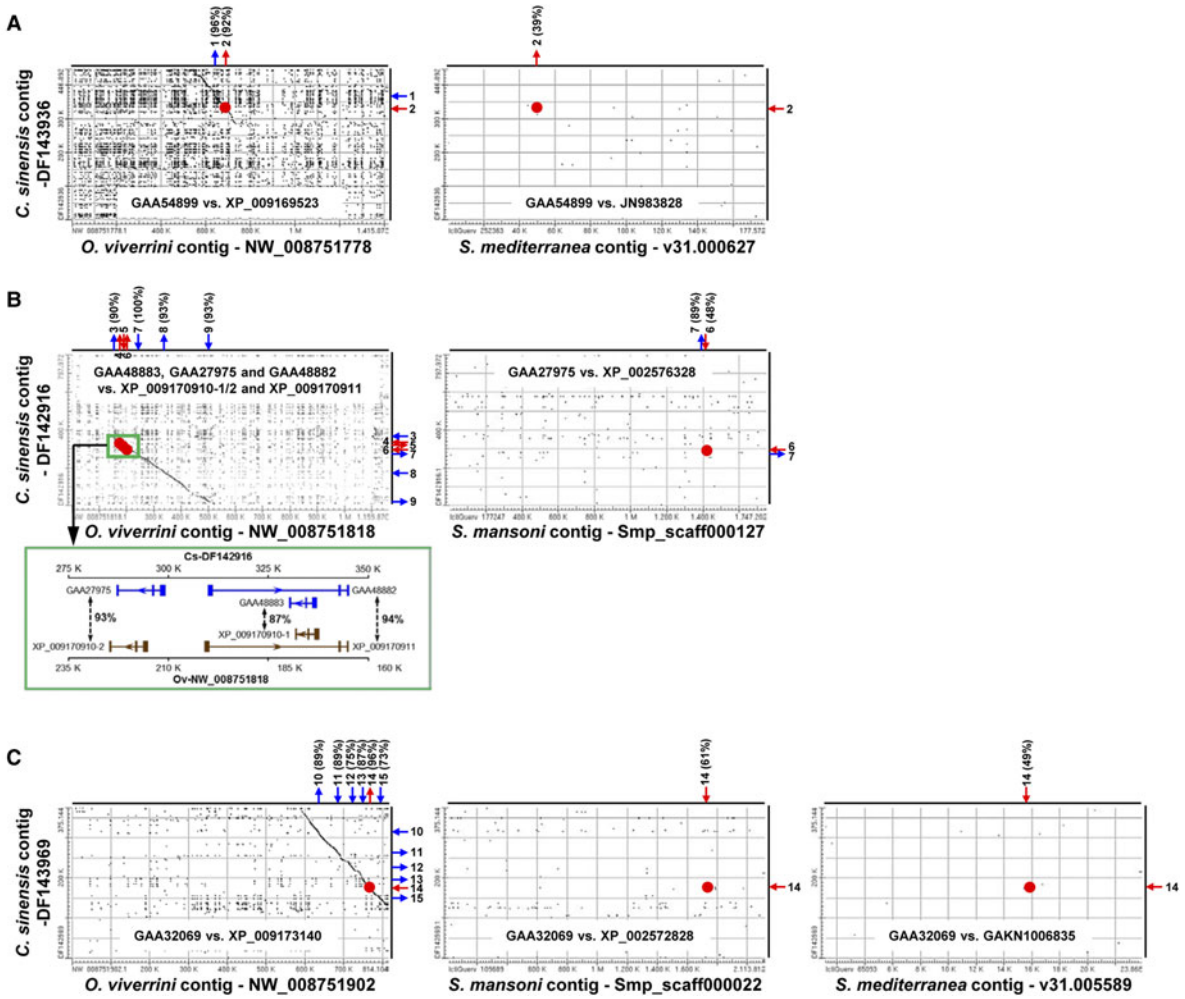

Fig. 4. Bl2seq alignments of the genomic regions encompassing platyhelminth tyrosinase genes belonging to the P_clade 1 (A), P_clade 2-A (B) and P_clade 2-B (C). The Bl2seq analyses were performed using tyrosinase-containing genomic contigs of *Clonorchis sinensis* (y axes) and their orthologous chromosomal segments in *Opisthorchis viverrini*, *Schistosoma mansoni*, and *Schmidtea mediterranea* (x axes). Syntenic genes detected in the *C. sinensis* (right y axes) and other platyhelminth (upper *x*-axes) contigs are marked with blue or red (tyrosinase) arrows, for which the direction reflects relative orientation of respective gene: 1, protein RMD5 homolog A; 2, tyrosinase; 3, NADH dehydrogenase (ubiquinone) 1 alpha; 4, tyrosinase; 5, tyrosinase; 6, tyrosinase; 7, large subunit ribosomal protein L31e; 8, protocadherin Fat 1; 9, hypothetical protein; 10, death-associated protein kinase 1; 11, testicular acid phosphatase homolog; 12, lysosomal acid phosphatase; 13, eggshell protein (TES superfamily); 14, tyrosinase; and 15, insulin receptor tyrosine kinase. Percentage identities between the *C. sinensis* proteins and their orthologs are also presented on the upper *x*-axes. Tyrosinase positions are marked with red circles on the diagonal lines exhibiting significant matches between the compared genomic contigs. The diagram in a green box depicts a comparison of genomic order between the *C. sinensis* and *O. viverrini* tyrosinases belonging to the P_clade 2-A.

these exogenous factors (Fig. 6B). The effect of bile on the expression level of tyrosinase genes could not be determined with the 7- and 12-day-old worms, because it was extremely difficult to collect sufficient worms for the experimentation.

DISCUSSION

The egg is the central resource responsible for the transmission and propagation of parasitic trematodes in an ecosystem that includes human populations. The agent also comprises the major etiological factors related to the generation of pathobiological changes in infected individuals (Cho *et al*. 2000; Hoffmann *et al*. 2002; Fairfax *et al*. 2012). Therefore, any strategy that aims to reduce parasite fertility may be highly effective for both the control of parasite transmission and the abatement of clinical symptoms induced by the parasite infection. We had previously investigated the structural and biochemical properties of four tyrosinase genes, which were identified in our EST database, and their role associated with egg formation in *C. sinensis* (Bae *et al*. 2013). The recent completion of the *C. sinensis* genome draft (Wang *et al*. 2011) allowed us to detect a fifth tyrosinase sequence (GAA54899), of which amino acid sequence had been incorporated into a phylogenetic analysis (Aguilera *et al*. 2013). In the present study, we primarily focused our analysis on the evolutionary features of *C. sinensis*

https://doi.org/10.1017/S003118201700083X Published online by Cambridge University Press

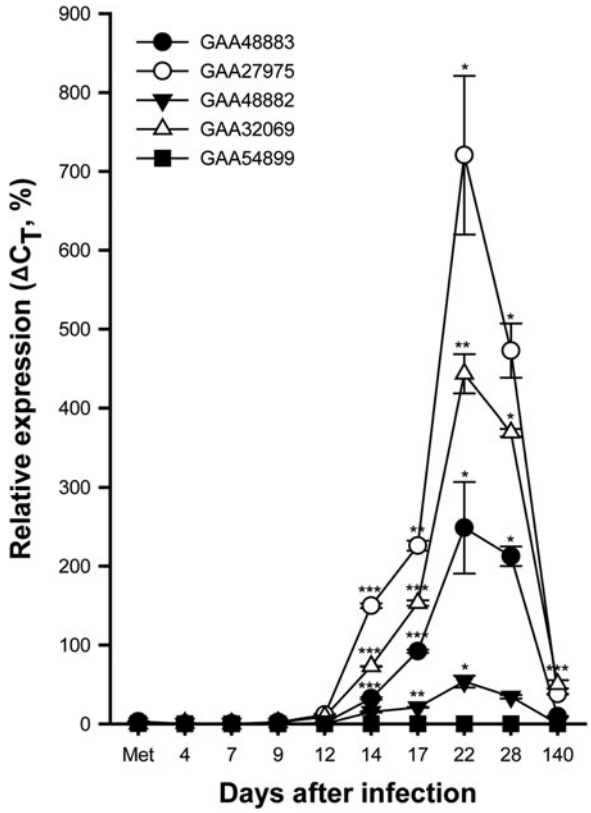

Fig. 5. Expression profiles of the *Clonorchis sinensis* tyrosinase genes during development/maturation of the parasite. Relative amounts of the respective tyrosinase transcripts were measured in total RNAs extracted from whole *C. sinensis* worms at various developmental stages, as indicated in the graph legend, by qRT-PCR. The calculations are based on the independent technical triplicates ($n = 3$, mean ± S.D.). The significance of expression change at a certain stage was statistically tested by comparing the expression level with that of the previous stage using the Student's *t*-test. *P* value, *<0·05; **<0·01; and ***<0·001.

tyrosinases with respect to their platyhelminth orthologs, in addition to their induction profiles against exogenous stimuli.

Like neodermatan flatworms such as trematodes, monogeneans and pseudophyllidean cestodes (Shinn, 1993; Swiderski and Xylander, 2000), free-living turbellarians and marine polychaete annelids depend on tyrosinase for the formation of sclerotized eggshells (Eckelbarger and Grassle, 1983; Ishida and Teshirogi, 1986; Shinn, 1993). In contrast, the advanced cyclophyllidean cestodes generate a keratin-type eggshell cross-linked by disulphide linkage (Arfin and Nizami, 1986). The phylogenetic distribution of the γ-subclass tyrosinases closely mirrored that of sclerotin-type eggshells across lophotrochozoans (Fig. 2). The subclass members were identified in trematodes (*C. sinensis*, *F. hepatica*, *O. viverrini*, *P. wertermani* and *Schistosoma* spp.), pseudophyllidean (*S. erinaceieuropaei*), triclad (*S. mediterranea*), and polychaete (*C. teleta*). However, no orthologous genes were identified within the genome drafts of taeniid cestodes including *E. multilocularis* (10× coverage, mapping of 89% sequences on the respective chromosomes; Tsai *et al.* 2013), as was previously predicted at the protein level (Smyth and McManus, 1989 and references therein). Interestingly, the marine demosponge *S. domuncula* (phylum Porifera) also expressed the γ-subclass tyrosinase, whereas equivalent genes were not identified in early metazoans such as *T. adhaerens* (Placozoa) and *N. vectensis* (Cnidaria). The sponge protein was likely to be involved in the production of the protocatechuate molecule for the energy metabolism of symbiotic bacteria (Müller *et al.* 2004). Taken together, these results suggest that the tyrosinase genes have undergone expansions and losses specific to the lineages of parasitic neodermatans.

The numbers of tyrosinase paralogs differed among platyhelminth species: six genes in the order Tricladida (*S. mediterranea*), five genes in the Opisthorchiida (*C. sinensis and O. viverrini*) and two genes in the Strigeidida (*Schistosoma* spp.) and Plagiorchiida (*F. hepatica*). The branching patterns in the phylogenetic trees demonstrated that these tyrosinase genes might have been duplicated at least three times before the divergence of turbellarian and neodermatan lineages (marked by solid diamonds in Fig. 2 and Supplementary Fig. 2). The last duplication resulted in generation of the two main paralog lineages detected in trematode species (P_clade 2-A and P_clade 2-B). The earlier duplication events appeared to have been accompanied by both the loss of one of resulting paralogs and the acquisition of novel exon-intron configurations (Fig. 3). Considering that the Strigeidida has diverged from other trematode lineages including the Plagiorchiida and Opisthorchiida during an early evolutionary phase (e.g. see Yang *et al.* 2015), the P_clade 1-lineage genes were likely to have been deleted independently in each of the neodermatan genomes, except for those in opisthorchiids. However, the *S. mediterranea* genes, especially the GAKN01005471 gene and P-clade 2-C members (GAKN01000997 and GAKN01001049), made this evolutionary scenario somewhat ambiguous. Future investigations that include tyrosinase genes in turbellarians comprising the Macrostomida, Polycladida and Tircladida (other than *S. mediterranea*), as well as monogeneans, would further clarify lineage-specific expansions and/or losses of tyrosinase genes across the Platyhelminthes.

The metacercaria of *C. sinensis* excysted in the duodenum of definitive host migrates directly into the bile ducts through the ampulla of Vater (Kim *et al.* 2011), where the parasite develops male and female sex organs as early as 7 dpi in experimental rats. Following the sexual maturation, the worm begins to express the tyrosinase and eggshell precursor protein genes coinciding with generation of the

https://doi.org/10.1017/S003118201700083X Published online by Cambridge University Press

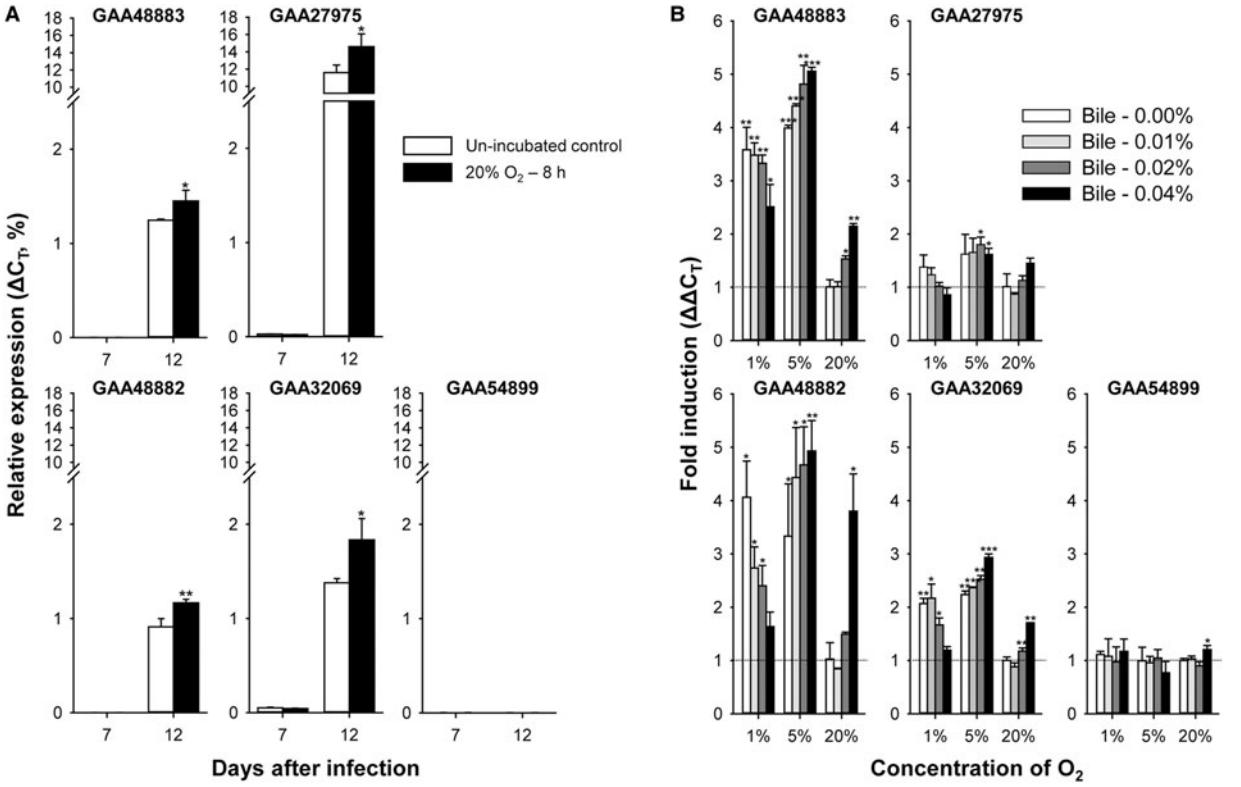

Fig. 6. Effects of oxygen and bile on the expressions of *Clonorchis sinensis* tyrosinase genes. (A) The 7- and 12-day-old worms were incubated for 8 h under 20%-O_2 conditions. Relative expression levels of tyrosinase genes were compared with those observed in un-incubated worms of the same age by qRT-PCR. (B) The 28-day-old worms were incubated in media supplemented with various amounts of bile for 8 h under 1-, 5- and 20%-O_2 conditions before tyrosinase expression levels were examined by qRT-PCR. The expression changes were presented as fold inductions compared to those in un-incubated control worms of the same age. The calculations are based on the independent technical triplicates ($n = 3$, mean ± S.D.). The significance of expression changes following exogenous stimuli was statistically tested by comparing the expression levels or fold inductions with those in the un-incubated control groups using the Student's *t*-test. *P* value, *<0·05; **<0·01; and ***<0·001.

tanned uterine eggs (Bae *et al*. 2013; Fig. 5). In *F. hepatica* that also sexually matures in the bile duct, multiple physicochemical factors such as bile, which are specific to the ductal environment, have been proposed as triggers for the sexual maturation/reproduction (Robinson *et al*. 2001; Hanna *et al*. 2006). In 28-day-old *C. sinensis* adult, the tyrosinase gene expressions showed a tendency to increase in response to *ex host* bile treatment. This inductive response was repeatedly observed in worms incubated under 20%-O_2 condition (Fig. 6B). Taken together the negligible levels of tyrosinase induction in 7-day-old worms stimulated with 20% O_2 (Fig. 6A), which also thrive in the bile ducts and lack of tyrosinase expression in metacercariae treated with bile (our un-published data), it seemed apparent that host bile does not act as the initial trigger, but serves to further up-regulate expression of tyrosinase genes. The results obtained with 7-day-old worms further indicated that the development of sexual organs is completed prior to the induction of tyrosinase genes, even though the main factors that initiate the developmental process are currently unknown (Bae *et al*. 2013; Figs 5 and 6). Bile and O_2 might affect only those worms with fully developed sex organs to induce the vitellocyte-specific tyrosinase genes.

Evolutionary events affecting eggshell formation-related genes are likely to be significantly influenced by the host and/or natural environments encountered by parasite's eggs to maximize the survival rates of fertilized ova/developing embryos. Eggs of most platyhelminths including trematodes and pseudophyllidean cestodes hatch in external aquatic environments, whereas those of cyclophyllidean cestodes hatch within their intermediate hosts (Shinn, 1993). Therefore, cyclophyllidean cestodes have developed a molecular mechanism to generate a thin keratin-type eggshell, which is easily broken down by mammalian digestive secretions, rather than conserving the ability to produce a sclerotin-type eggshell (Johri, 1957). This evolutionary process seems to have been accompanied by the loss of tyrosinase genes in the genomes of advanced cestodes. Considering the roles of eggs in tissue-invading helminths, our data regarding the evolution of tyrosinase genes among parasitic flatworms, as well as the induction profiles of *C. sin*ensis tyrosinases, could be

https://doi.org/10.1017/S003118201700083X Published online by Cambridge University Press

applicable in egg production-related control strategies for parasitic diseases including clonorchiasis.

SUPPLEMENTARY MATERIAL

The supplementary material for this article can be found at https://doi.org/10.1017/S003118201700083X.

ACKNOWLEDGEMENTS

The authors would like to express their profound gratitude to Professor Woon-Mok Shon of the Department of Parasitology, Gyeongsang University School of Medicine, Korea for their generous provision of *C. sinensis* metacercariae.

FINANCIAL SUPPORT

This work was supported by the Basic Science Research Program of the National Research Foundation of Korea (NRF), which was funded by the Ministry of Science, ICT and Future Planning (NRF-2013R1A1A2012011).

REFERENCES

Abascal, F., Zardoya, R. and Posada, D. (2005). ProtTest: selection of best-fit models of protein evolution. *Bioinformatics* **21**, 2104–2105.

Aguilera, F., McDougall, C. and Degnan, B. M. (2013). Origin, evolution and classification of type-3 copper proteins: lineage-specific gene expansions and loss across the metazoa. *BMC Evolutionary Biology* **13**, 96.

Andreini, C., Banci, L., Bertini, I. and Rosato, A. (2008). Occurrence of copper proteins through the three domains of life: a bioinformatics approach. *Journal of Proteome Research* **7**, 209–216.

Arfin, M. and Nizami, W. A. (1986). Chemical nature and mode of stabilization of eggshell/capsule of some cyclophyllidean cestodes. *Journal of Helminthology* **69**, 105–112.

Bae, Y. A., Cai, G. B., Kim, S. H., Sohn, W. M. and Kong, Y. (2013). Expression pattern and substrate specificity of *Clonorchis sinensis* tyrosinases. *International Journal for Parasitology* **43**, 891–900.

Bae, Y. A., Kim, S. H., Ahn, C. S., Kim, J. G. and Kong, Y. (2015). Molecular and biochemical characterization of *Paragonimus westermani* tyrosinase. *Parasitology* **142**, 807–815.

Bouvard, V., Baan, R., Straif, K., Grosse, Y., Secretan, B., El Ghissassi, F., Benbrahim-Tallaa, L., Guha, N., Freeman, C., Galichet, L. and Cogliano, V.: WHO International Agency for Research on Cancer Monograph Working Group (2009). A review of human carcinogens – part B: biological agents. *Lancet Oncology* **10**, 321–322.

Burmester, T. (2002). Origin and evolution of arthropod hemocyanins and related proteins. *Journal of Comparative Physiology* **172**, 95–107.

Cai, G. B., Bae, Y. A., Zhang, Y., He, Y., Jiang, M. S. and He, L. (2009). Expression and characterization of two tyrosinase from the trematode *Schistosoma japonicum*. *Parasitology Research* **104**, 601–609.

Cho, S. Y., Kong, Y., Yun, D. H., Kang, S. Y., Kim, L. S., Chung, Y. B. and Yang, H. J. (2000). Persisting antibody reaction in paragonimiasis after praziquantel treatment is elicited mainly by egg antigens. *Korean Journal of Parasitology* **38**, 75–84.

Cordingley, J. S. (1987). Trematode eggshells: novel protein biopolymers. *Parasitology Today* **3**, 341–344.

Decker, H. and Tuczek, F. (2000). Tyrosinase/catecholoxidase activity of hemocyanins: structural basis and molecular mechanism. *Trends in Biochemical Sciences* **25**, 392–397.

Eckelbarger, K. J. and Grassle, J. P. (1983). Ultrastructural differences in the eggs and ovarian follicle cells of *Capitella* (Polychaeta) sibling species. *Biological Bulletin* **2**, 379–393.

Edgar, R. C. (2004). MUSCLE: multiple sequence alignment with high accuracy and high throughput. *Nucleic Acids Research* **32**, 1792–1797.

Esposito, R., D'Aniello, S., Squarzoni, P., Pezzotti, M. R., Ristoratore, F. and Spagnuolo, A. (2012). New insights into the evolution of metazoan tyrosinase gene family. *PLoS ONE* **7**, e35731.

Fairfax, K. C., Amiel, E., King, I. L., Freitas, T. C., Mohrs, M. and Pearce, E. J. (2012). IL-10R blockade during chronic *Schistosomiasis mansoni* results in the loss of B cells from the liver and the development of severe pulmonary disease. *PLoS Pathogens* **8**, e1002490.

Fitzpatrick, J. M., Hirai, Y., Hirai, H. and Hoffmann, K. F. (2007). Schistosome egg production is dependent upon the activities of two developmentally regulated tyrosinases. *FASEB Journal* **21**, 823–835.

Guindon, S., Dufayard, J. F., Lefort, V., Anisimova, M., Hordijk, W. and Gascuel, O. (2010). New algorithms and methods to estimate maximum-likelihood phylogenies: assessing the performance of PhyML 3.0. *Systematic Biology* **59**, 307–321.

Hanna, R. E. B., Cromie, L., Taylor, S. M. and Couper, A. (2006). The effect of a parenteral ivermectin/closantel injection on the growth and reproductive development of early immature *Fasciola hepatica* in cattle. *Veterinary Parasitology* **142**, 78–90.

Hoffmann, K. E., Wynn, T. A. and Dunne, D. W. (2002). Cytokine-mediated host responses during schistosome infection: walking the fine line between immunological control and immunopathology. *Advances in Parasitology* **52**, 265–307.

Huang, X. and Madan, A. (1999). CAP3: a DNA sequence assembly program. *Genome Research* **9**, 868–877.

Ishida, S. and Teshirogi, W. (1986). Eggshell formation in polyclads (Turbellaria). *Hydrobiologia* **132**, 127–135.

Jaenicke, E. and Decker, H. (2004). Functional changes in the family of type3 copper proteins during evolution. *European Journal of Chemical Biology* **5**, 163–169.

Johri, L. N. (1957). A morphological and histochemical study of egg formation in a cyclophyllidean cestodes. *Parasitology* **47**, 21–29.

Keiser, J. and Utzinger, J. (2009). Food-borne trematodiases. *Clinical Microbiology Reviews* **22**, 466–483.

Kelly, D. H. and von Lichtenberg, F. (1970). "Abnormal" schistosome oviposition. Origin of aberrant shell structures and their appearance in human tissues. *American Journal of Pathology* **60**, 271–288.

Kim, T. I., Yoo, Y. G., Kwak, B. K., Seok, J. W. and Hong, S. J. (2011). Racing of the bile-chemotactic migration of juvenile *Clonorchis sinensis* in rabbits by PET-CT. *PLoS Neglected Tropical Diseases* **5**, e1414.

Livak, K. J. and Schmittgen, T. D. (2001). Analysis of relative gene expression data using real-time quantitative PCR and the $2^{-\Delta\Delta C}_{T}$ method. *Methods* **25**, 402–408.

Lun, Z. R., Gasser, R. B., Lai, D. H., Li, A. X., Zhu, X. Q., Yu, X. B. and Fang, Y. Y. (2005). Clonorchiasis: a key foodborne zoonosis in China. *Lancet Infectious Diseases* **5**, 31–41.

Mount, S. M. (1982). A catalogue of splice junction sequences. *Nucleic Acids Research* **10**, 459–472.

Müller, W. E. G., Grebenjuk, V. A., Thakur, N. L., Thakur, A. N., Batel, R., Krasko, A., Müller, I. M. and Breter, H. J. (2004). Oxygen-controlled bacterial growth in the sponge *Suberites domuncula*: toward a molecular understanding of the symbiotic relationships between sponge and bacteria. *Applied Environmental Microbioogy* **70**, 2332–2341.

Nicholas, K. B. and Nicholas, H. B., Jr. (1997). GeneDoc: a tool for editing and annotation multiple sequence alignments. Distributed by the authors. http://iubio.bio.indiana.edu/soft/molbio/ibmpc/genedoc-readme.html.

Page, R. D. (1996). Tree view: an application to display phylogenetic trees on personal computers. *Computer Applications in the Biosciences* **12**, 357–358.

Robinson, M. W., Colhoun, L. M., Fairweather, I., Brennan, G. P. and Waite, J. H. (2001). Development of the vitellaria of the liver fluke, *Fasciola hepatica* in the rat host. *Parasitology* **123**, 509–518.

Ronquist, F. and Huelsenbeck, J. P. (2003). MrBayes 3: Bayesian phylogenetic inference under mixed models. *Bioinformatics* **19**, 1572–1574.

Sánchez-Ferrer, A., Rodríguez-López, J. N., García-Cánovas, F. and García -Carmona, F. (1995). Tyrosinase: a comprehensive review of its mechanism. *Biochimica Biophysica Acta* **1247**, 1–11.

Shin, H. R., Oh, J. K., Masuyer, E., Curado, M. P., Bouvard, V., Fang, Y. Y., Wianqnon, S., Sripa, B. and Hong, S. T. (2010). Epidemiology of cholangiocarcinoma: an update focusing on risk factors. *Cancer Science* **101**, 579–585.

Shinn, G. L. (1993). Formation of egg capsules by flatworms (Phylum Platyhelminthes). *Transactions of the American Microscopical Society* **112**, 18–34.

Smyth, J. D. and Halton, D. W. (1983). *The Physiology of Trematodes*. Cambridge University Press, Cambridge.

Smyth, J. D. and McManus, D. P. (1989). *The Physiology and Biochemistry of Cestodes*. Cambridge University Press, Cambridge.

Swiderski, Z. and Xylander, W. E. R. (2000). Vitellocytes and vitellogenesis in cestodes in relation to embryonic development, egg production and life cycle. *International Journal for Parasitology* **30**, 805–817.

Tamura, K., Stecher, G., Peterson, D., Filipski, A. and Kumar, S. (2013). MEGA6: molecular evolutionary genetics analysis version 6.0. *Molecular Biology and Evolution* **30**, 2725–2729.

Tsai, I. J., Zarowiecki, M., Holroyd, N., Garciarrubio, A., Sanchez-Flores, A., Brooks, K. L., Tracey, A., Bobes, R. J., Fragoso, G.,

Sciutto, E., Aslett, M., Beasley, H., Bennett, H. M., Cai, J., Camicia, F., Clark, R., Cucher, M., De Silva, N., Day, T. A., Deplazes, P., Estrada, K., Fernández, C., Holland, P. W., Hou, J., Hu, S., Huckvale, T., Hung, S. S., Kamenetzky, L., Keane, J. A., Kiss, F., *et al*. (2013). The genomes of four tapeworm species reveal adaptations to parasitism. *Nature* **496**, 57–63.

van Gelder, C. W. G., Flurkey, W. H. and Wichers, H. J. (1997). Sequence and structural features of plant and fungal tyrosinases. *Phytochemistry* **45**, 1309–1323.

Wang, X., Chen, W., Huang, Y., Sun, J., Men, J., Liu, H., Luo, F., Guo, L., Lv, X., Deng, C., Zhou, C., Fan, Y., Li, X., Huang, L., Hu, Y., Liang, C., Hu, X., Xu, J. and Yu, X. (2011). The draft genome of the carcinogenic human liver fluke *Clonorchis sinensis*. *Genome Biology* **12**, R107.

Yang, X., Zhao, Y., Wang, L., Feng, H., Tan, L., Lei, W., Zhao, P., Hu, M. and Fang, R. (2015). Analysis of the complete *Fischoederius elongates* (Paramphistomidae, Trematoda) mitochondrial genome. *Parasites & Vectors* **8**, 279.

https://doi.org/10.1017/S003118201700083X Published online by Cambridge University Press